

<https://doi.org/10.1038/s42949-025-00302-z>

Multiple environmental inequalities between Global South and Global North in over 10,000 urban centers

Check for updates

Wei Li^{1,2}, Yongping Wei² ✉, Lijuan Chen³, Zhenjie Chen¹ ✉, Manchun Li¹ ✉, Wenqi Chen^{2,4}, Kunshu Yang², Diandian Xu⁵ & Qiqi Zhao^{1,6}

Our study assesses multiple environmental inequalities between the Global South and the Global North across more than 10,000 urban centers. Three environmental indicators (CO₂ emissions, air pollution (PM_{2.5}) and greenness) are used to represent three distinct environmental roles of urban ecosystems to society and human health, respectively: destruction (cost), victimization (harm) and contribution (benefit). The difference in relative importance, temporal dynamics, and driving patterns of these three indicators is analyzed between the Global South and the Global North. The results indicate that CO₂ emissions in the Global North exceed more than twice those in the Global South, whereas the mean PM_{2.5} concentration is less than half, reflecting significantly higher environmental destruction but lower environmental victimization. Global South and Global North exhibit similar trends in greenness, yet have different causes, with the luxury effect in Global North. Socioeconomic factors shape environmental development in the Global North, while both socioeconomic factors and natural endowments do so in the Global South. Achieving equitable environmental development of global urban centers requires breaking the development dilemma of the Global South and addressing the unequal exchange patterns between the Global North and the Global South.

Urban environmental inequalities not only pose a growing obstacle to achieving the United Nations Sustainable Development Goals (SDGs) but also undermine efforts to build inclusive, livable, and resilient urban environments¹. Urbanization—a global process—is reshaping landscapes, economies, and ecosystems across the planet^{2,3}. Yet this transformation manifests differently in the Global North and Global South^{4–6}. In the Global North, urbanization is typically accompanied by strong economic growth, extensive infrastructure, and improvements in public services. In contrast, in the Global South, urbanization is often incomplete. It is characterized primarily by the spread of impervious surfaces without proportional investments in economic, social, and infrastructural development. GDP per capita in the Global North was 12 times that of the Global South in 2022, doubling the disparity observed in 1950⁷. Urban built infrastructure per capita is also highly disproportionate, with some Global North countries surpassing those of Global South by more than 30-fold⁸. These differences in urbanization processes have created significant

environmental inequalities between the Global North and Global South^{9,10}.

The profound disparities between the Global North and the Global South are rooted in postcolonial urbanism. During the postcolonial period, the Global South continued to occupy a position of economic dependence and political subordination. These conditions gave rise to unequal ecological exchange, allowing the Global North to externalize its environmental costs¹¹. Specifically, the existing international mechanisms such as the Kyoto Protocol, the Copenhagen Accord, and the Paris Agreement allow the wealthy, high-emitting nations to continue “business as usual” for their carbon emission¹². The “pollution haven” phenomenon allows developed economies to relocate pollution-intensive industries to regions with lower environmental standards for surplus value while externalizing their environmental costs to the Global South¹³. Consequently, the harms of environmental destruction are disproportionately borne by low-income populations (Global South)¹¹. This structural mode of colonial

¹School of Geography and Ocean Science, Nanjing University, 210023, Nanjing, China. ²School of the Environment, The University of Queensland, Brisbane, 4072, Australia. ³Key Laboratory of Ecological Safety and Sustainable Development in Arid Lands, Northwest Institute of Eco-Environment and Resources, Chinese Academy of Sciences, 730000, Lanzhou, China. ⁴School of Public Affairs, Zhejiang University, 10058, Hangzhou, 3, China. ⁵School of Marine Science and Technology, Northwestern Polytechnical University, 710072, Xi'an, China. ⁶College of Geomatics, Xi'an University of Science and Technology, 710054, Xi'an, China. ✉e-mail: yongping.wei@uq.edu.au; chenzj@nju.edu.cn; limanchun@nju.edu.cn

appropriation casts the Global North as the “destroyer” and the Global South as the “victims”. Furthermore, while the reallocation of pollution-intensive industries aggravated the negative impact of the incomplete urbanization on greenness (“contribution”) in the Global South, wealthier societies not only mitigate environmental harms but also appropriate environmental amenities through processes such as green gentrification, reinforcing spatial and social inequalities in urban environments. Although this conceptual understanding of environmental inequalities between the Global North and the Global South is widely recognized, few studies have quantitatively assessed these inequalities.

Studies on environmental inequality, rooted in the sociological study of social inequality, refer to the uneven distribution of environmental benefits and harms, rewards and costs across social units such as individuals, groups, regions, and states^{14,15}. Environmental inequality is inherently a relative, dynamic and multi-dimensional concept, varying across time, space, and social categories¹⁶. Environmental justice, ecological modernization, and urban political ecology examine environmental inequality from different perspectives. Environmental justice focuses on the unequal distribution of pollution and environmental risks, highlighting the higher exposure of marginalized groups, such as low-income populations¹⁷; Yet it tends to overlook the multifunctionality of urban environments. Ecological modernization emphasizes technological and institutional innovation as ways to achieve a balance between economic growth and environmental protection¹⁸, but pays less attention to why cities develop differently within this process. Urban political ecology highlights how power relations and capital flows shape the production and distribution of urban environments. However, it remains largely conceptual and lacks a consistent indicator system and quantitative methods. These gaps compromise our capacity to mitigate the urban environmental inequality in the Global North and the Global South.

This study aims to assess multiple dimensions of environmental inequality between the Global South and the Global North across more than 10,000 urban centers. Drawing on theories of environmental inequality, complex socio-ecological systems, postcolonial thought, and urban political ecology, we develop a triadic destruction–victimization–contribution framework to measure environmental inequalities in urban centers. Within this framework, three environmental indicators—CO₂ emissions, air pollution (PM_{2.5}), and urban greenness—are employed to represent destruction (cost), victimization (harm), and contribution (benefit) to society and human health, respectively. Methodologically, we adopt three complementary analytical strategies. First, we assess the difference of the three urban environmental indicators between Global North and Global South by analyzing the relative importance of the three indicators with Ternary Diagram to identify their relative contribution to the entire environmental development; then, we track the temporal changes of the three indicators with a three-dimension (eight-quadrants) diagram to identify the change of their status (improved/degraded), and finally, we analyzed the driving patterns of the three indicators with structural equation modeling (SEM) to identify their causative chains (paths).

Results

Difference in three environmental indicators and their geographical and socio-economic drivers of urban centers between Global North and Global South

The distributional differences in the three environmental indicators and their geographic, social, and economic drivers between Global North and Global South were identified using the Mann-Whitney U test, to provide the basis for subsequent analyses. Environmental indicators of the urban centers show substantial differences between the Global North and the Global South, illustrated in Fig. 1 a–f. The global map of carbon emissions shows lower emissions in the Global South—particularly in Africa, India, and Southeast Asia—while much higher emissions are observed in North America, Europe, and East Asia. On average, carbon emissions per capita are 1.73 tons in the Global North, significantly higher than the 0.55 tons in the Global South. The global greenness map reveals that Europe, India,

Southeast Asia, Eastern North America and Central Africa are greener. Global North has a relatively higher mean greenness score (0.45) than Global South (0.40). Conversely, the air quality indicator shows higher PM_{2.5} levels in Asia and Africa. Global North has a lower mean PM_{2.5} concentration of 14.50 µg/m³ than Global South (38.77 µg/m³). In a word, Global North has twice higher mean CO₂, slightly higher greenness and twice lower mean PM_{2.5} than Global South while some urban centers in Global South present the case opposite to the mean values.

Urban socio-economic characteristics also reveal disparities, as shown in Fig. 1g–n. Global North has a higher average area per capita (250 m² per person) than Global South (45.8 m² per person). Furthermore, the average urban prosperity index in the Global North is 28.77, more than double the value of 10.46 in the Global South. The GDP distribution reveals significant regional disparities, as shown in Fig. 1k. North America, Europe, and Japan exhibit higher GDP values, while Africa displays lower values (Fig. 1l). The average GDP per capita in the Global North is \$18,377.47, significantly surpassing the Global South’s \$5,468.23. Global North has a higher mean and peak GDP distribution than Global South. However, the GDP per capita of a few urban centers in the Global South, such as the Greater Santa Cruz Area, Abu Dhabi, and Muhayil, exceeds that of some urban centers in the Global North. Global South’s GDP distribution forms a long tail, reflecting widespread income differences. Meanwhile, high-income regions (depicted in green in Fig. 1n) are mainly located in North America, Western Europe, East Asia (such as Japan and South Korea), as well as Australia and New Zealand. In contrast, middle- and low-income regions (orange, blue, and red in Fig. 1n) are concentrated in Latin America, South Asia, Southeast Asia, and sub-Saharan Africa. Although Global North has fewer urban centers, it contains the highest proportion of high-income-class (HIC) urban centers. The Global South has a larger number of lower-middle-income-class (LMIC) urban centers, followed by upper-middle-income-class (UMIC) urban centers, reflecting the region’s economic diversity. Overall, the Global North exhibits significantly higher socio-economic values, while the Global South presents greater variation in these indicators.

As one of the key geographic attributes, elevations in Asia, Europe, Africa, North America, South America, and Oceania are generally less than 1000 meters. They exceed 1000 m, however, in the high plateaus and mountain ranges of central North America, western South America, southern Africa, and the Tibetan Plateau region of Asia. On average, the elevation is 177.81 m in the Global North and 439.06 m in the Global South (Fig. 1o). The mean annual temperature is 11.34°C in the Global North and 22.00°C in the Global South. Similarly, the mean annual precipitation is 818.23mm in the Global North and 1144.80mm in the Global South. Overall, Global North exhibits significantly lower mean values for elevation, temperature, and precipitation relative to Global South.

Relative importance of the three environmental indicators between Global South and Global North

We analyze the differences in the relative importance of the three environmental indicators between the Global North and the Global South using a ternary diagram, in order to identify their contributions to overall environmental development. In the Global North, the mean values are 2.34 t a⁻¹ for CO₂ per capita, 1.40 × 10⁻⁴ µg m⁻³ for PM_{2.5} per capita, and 0.44 for greenness. After normalization, the percentage shares are 0.53 for CO₂, 0.05 for PM_{2.5}, and 0.42 for greenness. As a consequence of these share changes and the position of the dividing lines, the “high-contribution” zone contains the largest proportion of urban centers (24%). The “high-destruction” and “victimization–contribution trade-off” zones each account for 20%, both above the overall average. In contrast, the “high-victimization” zone is the smallest (10%), concentrated in the lower part of the diagram (Fig. 2a). The spatial map of the triadic environment contributions (Fig. 2c) shows that eastern North America and northern Europe in the Global North are “high-contribution areas”. Western North America, Japan, and Australia are “high-destruction areas”. Spatially, urban centers in the Global North are highly concentrated. The area within the 10th contour covers only 2.6% of

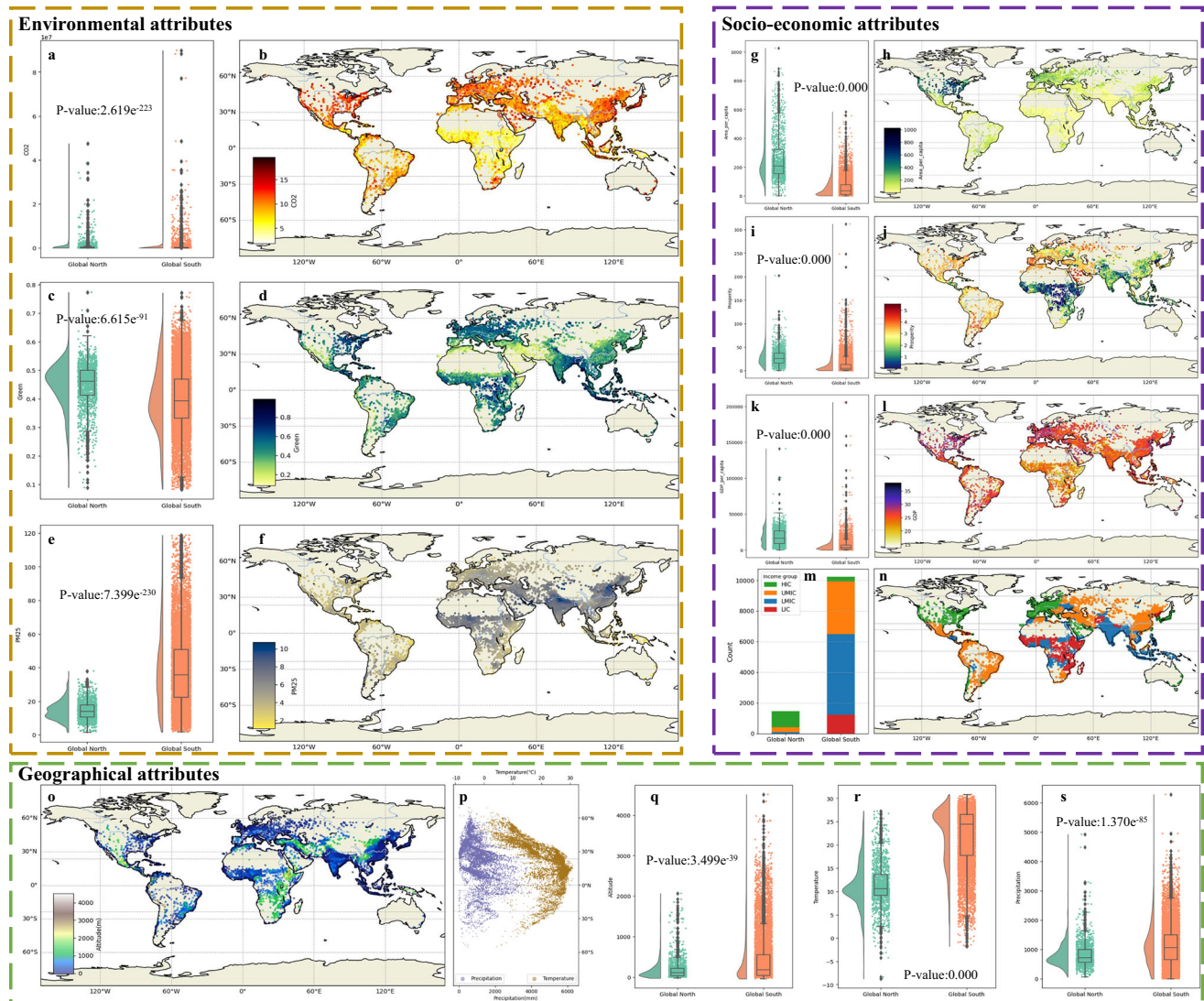


Fig. 1 | Differences in environmental, socio-economic, and geographical dimensions of urban centers between the Global North and Global South. **a** Difference of CO₂. **b** Distribution of global CO₂. **c** Difference of greenness. **d** Distribution of global greenness. **e** Difference of PM_{2.5}. **f** Distribution of global PM_{2.5}. **g** Difference of per capita area. **h** Distribution of per capita area. **i** Difference

of prosperity. **j** Distribution of global prosperity. **k** Difference of GDP per capita. **l** Distribution of global GDP per capita. **m** Difference of income group. **n** Distribution of global income group. **o** Distribution of global elevation. **p** Latitudinal distribution of global temperature and precipitation. **q** Difference of elevation. **r** Difference in temperature. **s** Difference in precipitation).

the map, while the highest densities surpass the 80th contour, reflecting a high degree of spatial consistency (Fig. 2a).

In the Global South, the mean values are 0.53 t a⁻¹ for CO₂ per capita, 3.70 × 10⁻⁴ μg m⁻³ for per capita PM_{2.5} concentration, and 0.40 for greenness. After normalization, the shares are 0.44 for CO₂, 0.15 for PM_{2.5}, and 0.41 for greenness. In terms of zonal distribution (Fig. 2b), the “high-destruction” and “high contribution” zones contain the largest shares of urban centers (22% and 21%, respectively). The “destructive-contributing trade-off” zone has the smallest share (13%), with other zones averaging around 15%. In the Global South, central Africa, Southeast Asia, and India are in the “high-contribution areas”. The “high-destruction areas” are mainly located in East Asia, West Asia, South America, and northern Mexico (Fig. 2d). Unlike the Global North, urban centers in the Global South are more dispersed, with the area within the 10th contour covering 49% of the map, and the highest densities surpassing the 20th contour, indicating significant spatial heterogeneity.

Both Global North and Global South exhibit a substantially high share of CO₂, confirming the central role of CO₂ in shaping environmental development. Both regions have a similar share of “high contribution area”

(over 20%). They both show relatively low shares of PM_{2.5}, but the magnitudes differ markedly: 0.05 in Global North compared with 0.15 in Global South, a difference of 10%. Spatial patterns also differ sharply. While the Global North has a concentrated urban distribution, the Global South is far more dispersed, with the 10th-contour area being 18.53 times larger than that of the Global North.

Difference in temporal development of the three environmental indicators between Global North and Global South

The differences in temporal changes of the three environmental indicators between the Global North and the Global South are analyzed using a three-dimensional (eight-quadrant) diagram. This approach identifies whether the indicators improved or degraded and assesses the relative ease of achieving environmental improvement, with Quadrant I representing the most favorable trajectory and Quadrant VIII the least favorable (Table 1). Overall, environmentally favorable quadrants (I, II, V) prevail in Global North (over 60%), whereas environmentally unfavorable quadrants (VI, VII, VIII) dominate in Global South (about 60%) (Table 1, Fig. 3). Per capita GDP in Global North (yellow–blue hues) is consistently higher than that of

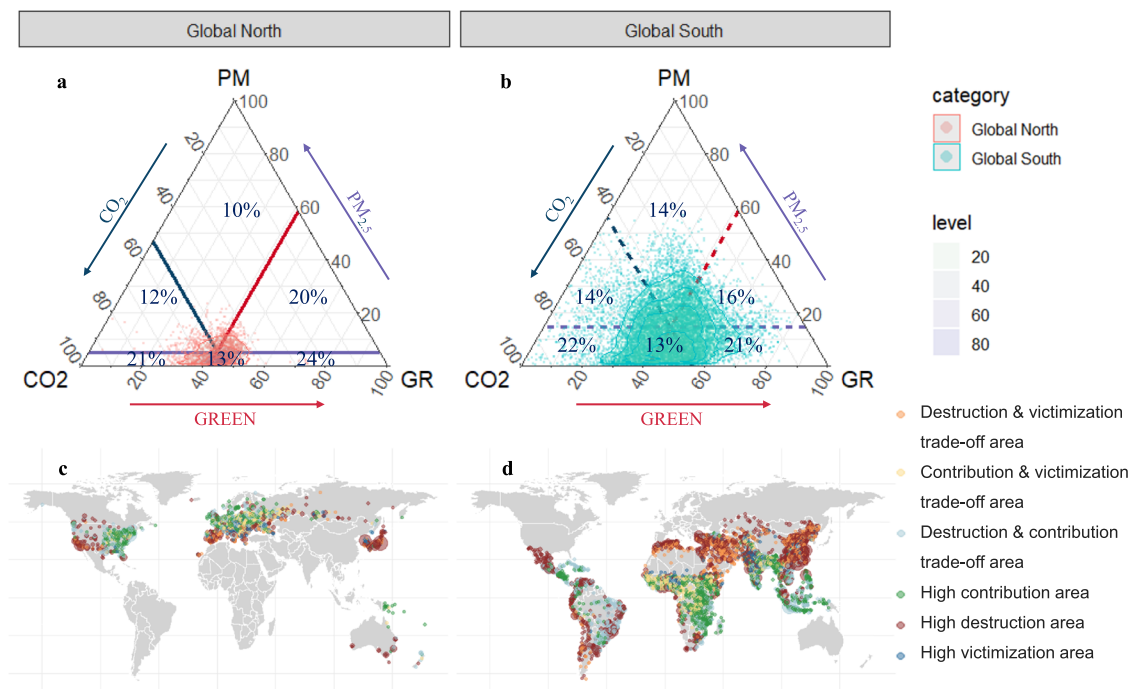


Fig. 2 | Urban environmental triangular contribution in Global North and Global South. a Global North. **b** Global South. Spatial distribution of the six areas. **c** Global North. **d** Global South).

Table 1 | Distribution of urban centers of Global North and Global South in the eight quadrants

Number of Scenario	Scenario situation	Global North (%) and main continents (countries)	Global South (%) and main continents (countries)
I	Synergy (best) (Improvement across all three environmental indicators)	13.08 North America, Japan, and parts of Europe	5.10 Mexico and South Africa
II	Trade-off; (improved CO ₂ emissions and PM _{2.5} concentration but worse greenness)	12.21 North America and Oceania	6.93 Colombia, Venezuela, and South Africa
III	Trade-off (improved CO ₂ emissions and greenness but worse PM _{2.5} concentration)	5.39 Japan	1.19 West Asia and Northeast China
IV	Trade-off (improved CO ₂ emissions but worse PM _{2.5} concentration and greenness)	2.54 Japan	1.87 West Asia
V	Trade-off (worse CO ₂ emissions but improved PM _{2.5} concentration and greenness)	35.59 eastern North America and western Europe	25.04 Mexico, Africa, and Asia
VI	Trade-off (worse CO ₂ emissions and greenness but improved PM _{2.5} concentration)	6.63 the American Southwest and Europe	26.23 South America and Asia
VII	Trade-off (worse CO ₂ emissions and PM _{2.5} concentration but improved greenness)	19.34 Eastern Europe	17.10 East Asia
VIII	Synergy (worst) (Deterioration across all three environmental indicators)	5.21 Eastern Europe and South Korea	16.53 West Africa, West Asia, and East Asia

Global South (orange–red hues). However, the Global South contains a greater number of megacities than the Global North, as indicated by a larger point size in Fig. 3.

Quadrant I (improvement across all three environmental indicators) accounts for 13.08% of Global North but only 5.10% of Global South. Northern cities in this quadrant are located in North America, Japan, and parts of Europe, with GDP per capita ranging from \$10,000 to \$20,000. Southern cities are found mainly in Africa, where a peak per capita GDP is \$500—one of the two lowest among all eight quadrants (the other being Quadrant III, which accounts for only 1%). In contrast, Quadrant VIII

(deterioration across all three environmental indicators) accounts for 5.21% of Global North and 16.53% of Global South. In the Global North, these cities are located in Eastern Europe and South Korea, with peak per capita GDP ranging from \$8,000 to \$10,000. In the Global South, they are distributed across West Africa, West Asia, and East Asia, with a peak per capita GDP of \$1000.

For quadrants where the three environmental indicators do not simultaneously improve or deteriorate, similarities and differences can be observed in both the Global North and the Global South. Quadrant V (worse CO₂ emissions but improved PM_{2.5} concentration and greenness) is the

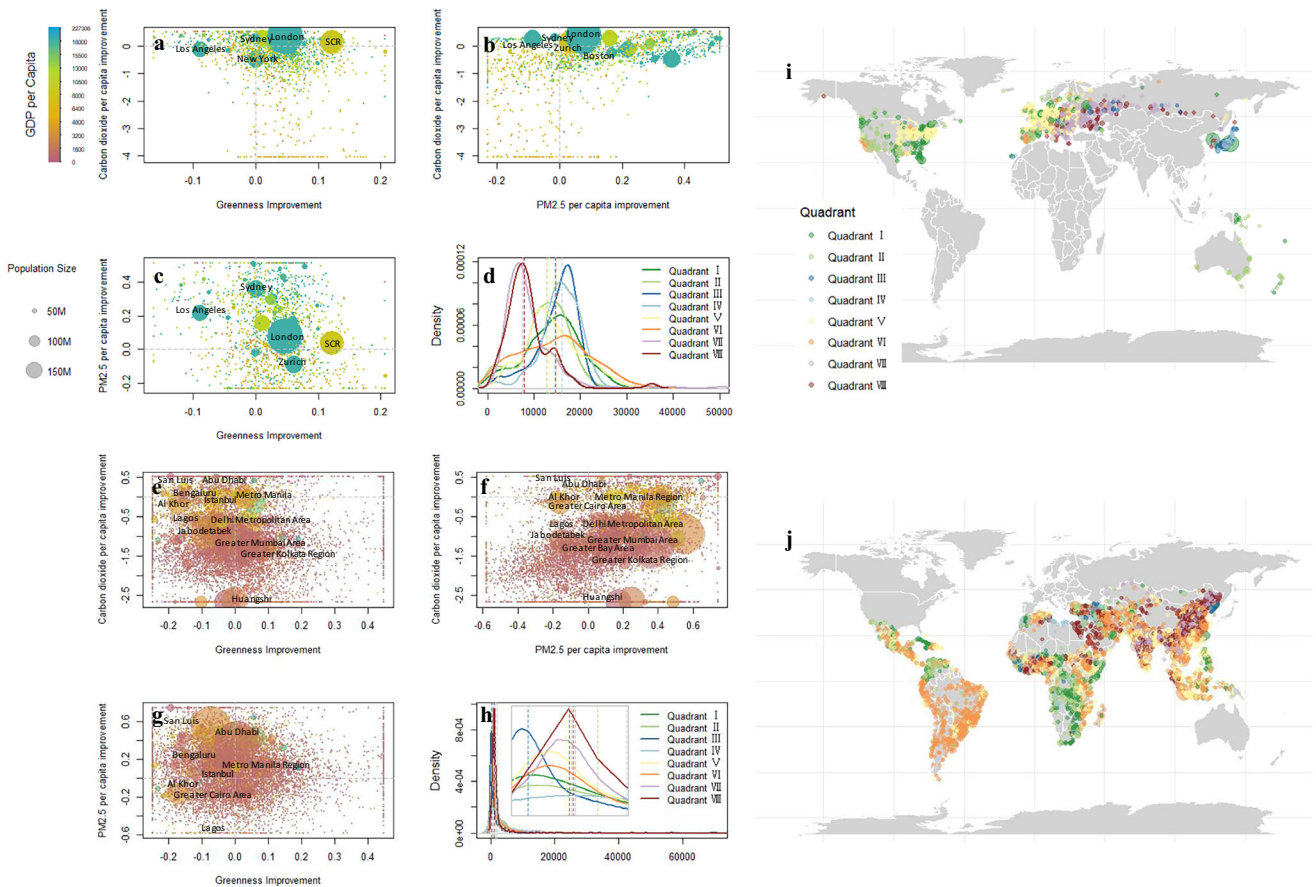


Fig. 3 | Environmental changes and socio-economic distribution in Global North and Global South. a Greenness vs Carbon Change of Global North. **b** $PM_{2.5}$ vs Carbon Emission Change of Global North. **c** Greenness vs $PM_{2.5}$ Change of Global North. **d** Distribution of GDP per capita density in eight quadrants of Global North. **e** Greenness vs Carbon Change of Global South. **f** $PM_{2.5}$ vs Carbon Emission Change

of Global South. **g** Greenness vs $PM_{2.5}$ Change of Global South. **h** Distribution of GDP per capita density in eight quadrants of Global South. **i** Distribution of Global North environmental changes. **j** Distribution of Global South environmental changes.

largest quadrant in Global North (35.58%), characterized by a peak GDP of \$10,000, and spatially concentrated in eastern North America and western Europe. In the Global South, Quadrant V accounts for 25.04%, with a peak GDP of only \$500, mainly concentrated in Mexico, Africa, and Asia. The largest quadrant in the Global South is Quadrant VI (improved air quality, but worse greenness and CO_2 emissions), accounting for 26.23%, compared with only 6.63% in the Global North. This quadrant is characterized by GDP levels below \$1500 and is concentrated in South America and Asia. Quadrant VII (worse CO_2 emissions and $PM_{2.5}$ concentration but improved greenness) has similar and relatively large proportions in the Global North (19.34%) and the Global South (17.10%). In the Global North, these cities have relatively low GDP levels (\$5000–\$10,000) and are mainly located in Eastern Europe. In the Global South, GDP levels skew toward the upper bound within the regional context, with a peak of about \$500, and these cities are mainly distributed across East Asia.

There are some distinct characteristics in terms of the relationship between greenness and development (CO_2 and $PM_{2.5}$) among continents. In Europe and North America, high CO_2 levels coexist with high greenness, where all three environmental indicators improve or only CO_2 worsens—an expression of luxury sustainability with hidden emissions. Latin America shows medium greenness with various but uneven development trajectories, reflecting fragmented urban governance. South Asia faces a “triple burden” of rising CO_2 , declining greenness, and severe $PM_{2.5}$ exposure, representing a case of vulnerability clustering. In East Asia, despite relatively high income levels within the Global South, economic benefits have been achieved at the cost of environmental degradation, with high CO_2 and $PM_{2.5}$ levels and continuous deterioration across all three indicators. Finally,

Southern Africa demonstrates high greenness and improving environmental contributions despite severe income disadvantages, marking it as a left-behind in the globalized system.

Difference in driving mechanism of environmental development between Global North and Global South

Differences in the driving patterns of the three environmental indicators between the Global North and the Global South are analyzed using SEM to reveal their causal chains (paths). In the Global North, CO_2 emissions are predominantly driven by economic, demographic, and geographic factors, with a high explanatory power of 69% (Fig. 4). GDP and urban area exert the strongest positive influence, followed by population. Geography plays a dual role, directly suppressing emissions while indirectly increasing them through GDP growth or land constraints. $PM_{2.5}$ has a lower explanatory power (29%), with population and income levels contributing positively, while carbon emissions mitigate $PM_{2.5}$. Population affects $PM_{2.5}$ both directly and indirectly through carbon emissions. Greenness, with an explanatory power of 14%, is negatively influenced by income and urban prosperity (−0.273 and −0.080), creating conflicting effects.

In the Global South, CO_2 patterns are similar to those in the Global North but with different factor influences, yielding an explanatory power of 62%. The population has a strong direct effect (0.414) and an indirect impact via GDP and built-up land. Geography restricts construction land but promotes income growth, which drives emissions. $PM_{2.5}$ has a weak explanatory power (5%), with income groups and greenness exerting negative effects (−0.122 and −0.023), while carbon emissions have a minor positive effect (0.047). Indirectly, income groups reduce greenness, reducing

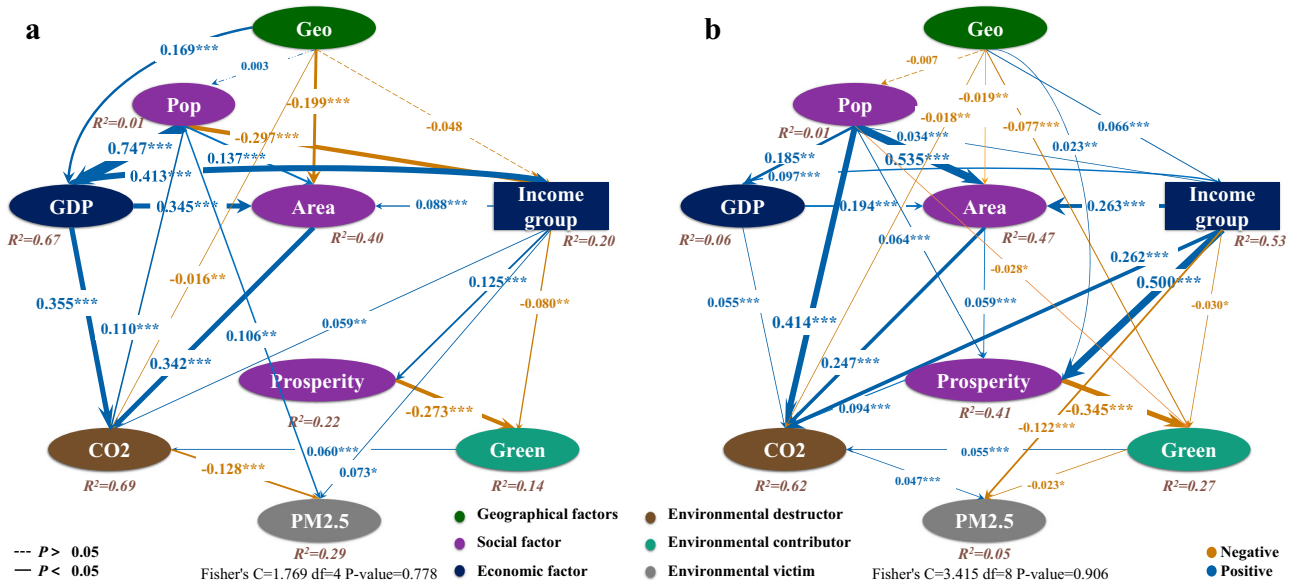


Fig. 4 | Driving patterns of urban environmental development. a Global North. **b** Global South.

PM_{2.5}, but also promote carbon emissions, increasing PM_{2.5}. Greenness, with an explanatory power of 27%, is negatively affected by geography, population, prosperity, and income, with prosperity having the strongest dampening effect (−0.345).

Taken together, these contrasts reveal systematic differences in the driving patterns of urban environmental development. In the Global North, population drives GDP, which in turn influences CO₂ emissions, while in the Global South, population directly drives CO₂ emissions. Both regions share the role of built-up land area in stimulating CO₂. Another path shared by both regions is the dampening effect of prosperity on greenness, which is less in the Global North than in the Global South. In addition, geography in the Global South also plays a role in greenness. The population in the Global North influences PM_{2.5}, but greenness in the Global South influences PM_{2.5}. In general, socioeconomic factors dominate environmental development in the Global North, while both socioeconomic factors and natural endowments together shape development in the Global South.

Discussion

Our results reveal statistically significant differences in the three environmental indicators and their geographic, social, and economic drivers across more than 10,000 urban centers between the Global North and the Global South. This aligns with Zhou et al.⁸ on GDP disparities, Nagendra et al.¹⁹ on urban prosperity, and Chen et al.²⁰ on the greater heterogeneity in the Global South.

The most pronounced environmental inequality is CO₂ emission (environmental destruction) between the Global North and the Global South, although both are in the direction of deterioration. The average CO₂ emission of the Global North is more than twice that of the Global South. In terms of temporal changes, both regions show increasing trajectories in CO₂ emissions. Consistent with Cheng et al.²¹, this may reflect the continued rise in greenhouse gas emissions from fossil fuel combustion and land use changes since the 19th century. We also find a strong correlation between CO₂ and socio-economic indicators, with the explanation of more than 60% in both Global North and Global South, aligning with Zheng et al.²² and Betts-Davies et al.²³. Rising CO₂ emissions are also partly driven by population expansion, particularly in low-income nations²⁴. The contribution of built-up land area to CO₂ is confirmed as the third global greenhouse gas emissions source²⁵. Finally, our results indicate that 27.88% of urban centers in the Global North show improved CO₂ emissions, compared with only 16.12% in the Global South. This disparity may be associated with regional differences in energy transitions²⁵. These findings reveal that the global

economy continues to develop at the expense of environmental sustainability and the ecological burden on the climate is being further intensified¹¹. In the Global South, environmental destruction is largely driven by a carbon-intensive development pathway based on fossil fuel dependence, population growth, and urban expansion²⁶. In contrast, in the Global North, it is at least partially fueled by the high-consumption lifestyles of affluent populations²⁷. Together, these dual trajectories exacerbate global climate risks, revealing that capitalist urbanization generates a shared but uneven ecological burden, locking both the Global North and the Global South into carbon-intensive pathways.

The secondary environmental inequality between the Global North and the Global South is PM_{2.5} exposure (environmental victimization). PM_{2.5} exposure in the Global North is less than half that in the Global South. Regions with high PM_{2.5} concentrations are mainly located in Asia and Africa. A larger share of urban centers falls into high-victimization areas in the Global South (14%) compared with the Global North (10%). Over time, 72.66% of urban centers in the Global North improved their PM_{2.5} levels, compared with only 62.63% in the Global South. Geographic and socioeconomic factors have low explanatory power for PM_{2.5} in both Global North (29%) and Global South (5%), indicating its causal complexity, in agreement with Li et al.²⁸, Yang et al.²⁹ and Behrer and Heft-Neal³⁰. In the Global North, Behrer and Heft-Neal³⁰ found that there was a “decoupling” of PM_{2.5} in developed countries: as urban centers continue to expand, PM_{2.5} concentrations decline. The industrial upgrading with the replacement of fossil fuels with cleaner energy and the relocation of polluting industries outside the Global North can explain it¹⁴. The explanatory power for PM_{2.5} in the Global South is notably low (5%), reflecting the complex and multi-scalar drivers of particulate pollution. PM_{2.5} levels are shaped not only by local geographic and socio-economic factors but also by regional atmospheric transport, climatic variability, and topographical influences, which can obscure the contribution of urban-scale drivers^{10,31}. Specifically, the interplay of transboundary transport, intra-Global South heterogeneity, divergent development pathways, and weak regulation driven by the pressure to grow its economy can collectively contribute to the lower explanatory power for PM_{2.5}. As a result, the Global South bears a disproportionate share of environmental harm.

The smallest environmental inequality is greenness (environmental contributions). Greenness is above 0.40 in both the Global North and the Global South. However, from 2000 to 2015, greenness has been improved in 74% of urban centers in the Global North and only 48% in the Global South. Geographic, social, and economic factors have low explanatory power for

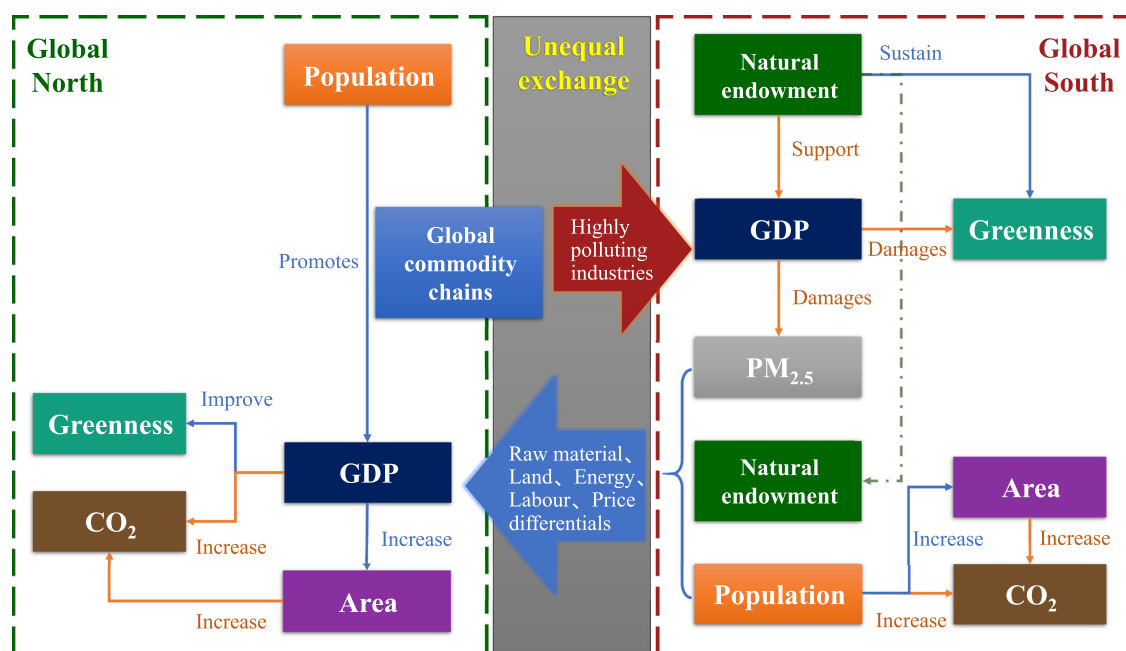


Fig. 5 | A conceptual model of the global North-South development patterns for explaining multiple environmental inequalities between Global North and Global South.

greenness in both the Global North (14%) and the Global South (27%). The first common recognition for this low explanation may be due to the heterogeneity of geography³². Then, the destruction and construction of green spaces can also occur periodically and are not always strictly chronological³³. Finally, there is a well-documented positive correlation between green space and wealth, known as the “luxury effect”³⁴. High greenness in the Global North coexists with high CO₂ emissions. This can reflect a form of “luxury sustainability”. By contrast, many cities in the Global South are located closer to the equator, which naturally leads to higher greenness³⁵. The simultaneous deterioration of CO₂ emissions and greenness may reflect rapid land conversion for urban expansion and urbanization, where infrastructural deficiencies exacerbate environmental pressures in the Global South^{36,37}. Therefore, there are different causes for the similar greenness in the Global North and the Global South.

The profound inequalities across the three environmental indicators between the Global North and the Global South are rooted in postcolonial urbanism. The developmental trajectory in the Global South remains marked by economic dependence, political subordination, and unequal ecological exchange¹¹. Specifically, the global unbalanced trade structure has led to a situation where resource and labor flows from the Global South—amplified by trade price differentials—substantially support the economic growth of the Global North^{38,39}. Meanwhile, some backward enterprises with high CO₂ emissions and other pollutants in developed countries have moved to the countries that need to develop their economies, thus leading to developing regions in the Global South becoming pollution havens^{13,40,41}. Meng et al.² confirmed that unequal exchange is a significant driver of global inequalities in environmental development, even ecological breakdown. This partly explains our finding that CO₂ in the Global North is strongly tied to economic development, whereas in the Global South it is more closely associated with population, with a greater share of urban centers becoming environmental victims. Based on the Red Ring-Green Ring model developed by Cumming, et al.⁴² and Cumming and von Cramon-Taubadel⁴³ and our SEM results, we propose a whole-of-system conceptual model for explaining root causes of the different driving patterns of multiple environmental inequalities between Global North and Global South (Fig. 5).

Figure 5 illustrates that urban environmental inequality is not an isolated phenomenon but a structural outcome of global urbanization. Urbanization is not a linear process of spatial expansion; rather, it unfolds through diverse social, political, and economic pathways, accompanied by

unequal patterns of resource use and ecological burden³⁶. In the Global North, economic growth has gradually “decoupled” from PM_{2.5}, partly as a result of technological innovation and green transitions. By contrast, in the Global South, industrial relocation and weak regulatory frameworks may have turned it into a “receiving zone” for pollution⁴⁴. Financial constraints often prioritize infrastructure directly linked to economic development, while facilities such as urban green spaces, hospitals, and other public amenities remain underprovided, producing a marked “infrastructure gap” with the Global North⁴⁵. Roy³⁷ characterizes this situation as a form of incomplete urbanization, where urban growth is driven primarily by expansion of the built environment rather than balanced social investment. Limited infrastructural capacity, coupled with uneven governance, may further exacerbate socio-ecological vulnerabilities¹⁹.

But encouragingly, while Global North has institutionally exported environmental harm, it is also actively working to mitigate damage. Global North has introduced carbon tariffs to curb high-carbon lifestyles from the consumption side²⁷. At the same time, the Global South is not merely a passive recipient of harm. It has proactively taken bottom-up actions within communities, including grassroots citizen participation, low-cost housing solutions, and collective action via social media, to mitigate environmental degradation¹⁹. In addition, international organizations, such as the World Bank, the World Food Programme, and the Global Facility for Disaster Reduction and Recovery (GFDRR), have been addressing environmental inequalities between the Global North and the Global South through financial support, data sharing, and policy instruments⁴⁶. These policy pathways align closely with the United Nations Sustainable Development Goals (SDGs)—particularly SDG 11.6, which emphasizes reducing the per capita environmental impact of cities (e.g., through improved air quality and waste management); SDG 13, which calls for urgent climate action; and SDG 10, which aims to reduce inequalities within and between countries. These findings provide an evidence base for prioritizing interventions that directly support these goals, particularly by identifying where destruction, victimization, and contribution dynamics are most pronounced.

Obviously, further policy is needed to address the significant environmental inequalities. In Europe and North America (Quadrants I, II, and V), the central challenge lies in high consumption and the outsourcing of hidden emissions. A progressive carbon tax on affluent high-consumption groups, designed around emission levels, could provide an effective corrective mechanism²⁷. South Asia (VIII) faces a triple burden cluster of rising

CO₂, declining greenness, and severe PM_{2.5} exposure. An integrated policy package including subsidies is required to assist this region in escaping from the locked-in predicament. In trade-off situations where economic growth occurs at the expense of environmental degradation (for example, East Asia in Quadrants VI, VII, and VIII) or where high levels of urban greenness are maintained under extremely low-income conditions (for example, Southern Africa in Quadrants I, II, and V) (Table 1), difficult prioritization decisions are often required. However, certain co-benefit interventions can help balance competing objectives. Urban green infrastructure, such as green roofs, vertical greening, and nature-based stormwater management systems^{47–49}, can simultaneously reduce carbon emissions, improve air quality, and enhance urban greenness, thereby generating multiple environmental and social benefits. In the long term, achieving environmentally balanced development in global urban centers will require breaking the development dilemma facing the Global South and reshaping the unequal exchange relationship between the Global North and the Global South, as illustrated in Fig. 5. This transformation can ensure a more equitable distribution of environmental benefits.

This study develops a novel triad destruction–victimization–contribution framework for measuring environmental inequalities in urban centers in which we employ greenness, PM_{2.5} concentration, and CO₂ emissions as proxies for environmental contribution, victimization, and destruction, respectively. This framework captures the relative roles of CO₂, PM_{2.5}, and greenness in shaping urban environmental inequality rather than to measure their absolute impacts or only to use one single indicator. It contributes to the improvement of three related disciplines: environmental justice, ecological modernization, and urban political ecology in understanding the environmental inequalities. Methodologically, this study offers new tools to develop pathways toward fairer and more sustainable urban futures. It should be noted that as CO₂, PM_{2.5}, and greenness represent different socio-ecological processes, this study assigned equal weights to them, providing a neutral baseline that avoids dominance by any single dimension. The different weights may be used to different urban environmental contexts and different policy foci, e.g. emphasizing CO₂'s global responsibility, prioritizing PM_{2.5} for environmental health risks, or underscoring equal access to greenness. They could cause the change of positions of urban centers in the ternary space thus reclassification of and structural changes in urban centers.

However, this study has certain limitations, as the structural equation model did not account for spatial autocorrelation in the global dataset. If inadequately treated, spatial dependence can lead to statistical problems such as inflated Type I error rates, biased parameter estimates, and spatially structured residuals^{50,51}. Future work could address this by adopting computationally efficient approaches such as spatial eigenvector mapping⁵² or spatial filtering. In addition, further research should develop a more nuanced typology of Global South regions by accounting for intra-regional heterogeneity (for instance, differences between South Asia and Sub-Saharan Africa) to avoid that the results are overly generalized. Subsequent work should also expand the range of geographic and socioeconomic indicators, incorporate longer time-series data and explore feedback mechanisms and the constraints imposed by tipping points to deepen understanding of system dynamics under different development pathways.

Methods

Data source

The Global Human Settlement Urban Centre Database (GHS-UCDB) was used in this study, covering over 10,000 urban centers in various areas across the globe⁵³. This database includes data on geography, socio-economics, environment, disaster risk reduction, and sustainable development, as well as the location and extent of each urban centre, covering 1990, 2000, and 2015. It is generated by integrating rich geospatial data provided under open data policies and new Earth observation programs, such as the Copernicus program. The Global Human Settlement Layer (GHSL) project delineates urban centers using the “Degree of Urbanization” method based on population density and built-up area thresholds. Utilizing Geographic

Information System (GIS) technologies, multi-thematic and multi-temporal variables are linked to these urban centers through methods like zonal statistics and spatial analysis, with quality ensured via high-resolution imagery verification. Therefore, this database offers researchers a robust foundation for examining complex urban phenomena at a regional and global scale.

Global South includes urban centers in South America, Africa and parts of Asia, while Global North includes urban centers in North America, Europe, Australia, and developed Asia⁴⁵. Among the 11,683 urban centers in the database, there are 10,070 urban centers in the Global South, accounting for 86.2% of the urban centers, while 1,613 urban centers in the Global North, account for 13.8% of the global urban centers. For instance, in the Global South, urban centers such as São Paulo and Rio de Janeiro in South America, Lagos and Nairobi in Africa, and Mumbai and Jakarta in Asia are representative examples. In the Global North, typical urban centers include New York and Toronto in North America, London and Paris in Europe, Sydney and Melbourne in Australia, as well as Tokyo and Seoul in developed Asia.

A triadic destruction–victimization–contribution framework for assessing environmental inequalities in urban centers and identifying their determinants

We, built upon interdisciplinary understandings of urban environmental equality's multidimensionality and urban ecosystem complexity, for the first time, develop a triadic destruction–victimization–contribution framework of measuring environmental inequalities in urban centers. In this framework, CO₂ emissions are used to represent environmental destruction, as it is a dominant form of environmentally damaging activity that is deeply intertwined with human economic development²⁵. CO₂ emission is a direct byproduct of fossil fuel–based industrialization and consumption, and it drives global climate change, ocean acidification, and biodiversity loss. Crucially, this form of environmental destruction has become a privilege under postcolonial power structures over environmental responsibility²⁷. PM_{2.5} concentration is selected as a proxy for environmental victimization. Fine particulate matter is one of the most harmful air pollutants, with disproportionate exposure observed among marginalized urban populations¹⁷. PM_{2.5} represents the local and immediate impacts of environmental degradation, particularly on public health^{54,55}. It represents how environmental risks are unevenly distributed and disproportionately borne by the most vulnerable, which is central to environmental justice and urban political ecology. Greenness captures environmental contribution. As an indicator of positive ecological intervention, greenness reflects local efforts to improve environmental quality through carbon sequestration, urban cooling, pollution mitigation, and health promotion⁵⁶. In addition, it plays a dual role—it not only contributes to mitigating PM_{2.5} concentrations⁵⁷, but also serves as a key strategy for combating global warming⁹. Thus, greenness links to the other two dimensions, offering a practical means of transforming victimization and destruction into contribution.

Building on insights from complex systems theory and urban political ecology⁵⁸, we conceptualize the urban environment as a coupled socio-ecological system whose dynamics emerge from the nonlinear interactions among its multiple subsystems. Environmental development is jointly shaped by geographical endowments and socio-economic drivers.

Geographical indicators included in this paper are temperature, precipitation, and elevation, which primarily represent natural endowments and express the geographic and climatic context of urban centers. Social indicators include built-up area and prosperity measured by nighttime light intensity, which mainly reflect urban spatial organization and the intensity of human activities. Economic indicators include per capita GDP and income group classifications, which primarily indicate the level of economic development and wealth distribution (Table 2). Nighttime light intensity is included as a proxy for economic activity and urban prosperity, following Zhai et al.⁵⁹, who demonstrated its effectiveness in capturing urban–rural economic dynamics. Previous studies have also visually confirmed the

Table 2 | Overview of variables used in this study

Variable name	Symbol	Unit
CO2	CO2	t a ⁻¹
Greenness	Green/GR	Unitless
PM2.5	PM2.5/PM	µg m ⁻³
Elevation	Geo	M
Temperature	Geo	°C
Precipitation	Geo	Mm
Population	Pop	Unitless
Build up area	Area	km ²
Nightlight	Prosperity	nW cm ⁻² sr ⁻¹
GDP	GDP	\$
Income group	Income group	Unitless

correspondence between nightlight patterns and human settlement/economic activity.

Analysis of the three environmental inequalities of the urban centers between Global North and Global South

Data preprocessing: Records containing missing values for any of the key indicators were excluded to maintain consistency across all variables. To reduce potential bias and enhance the robustness of the results, extreme outliers were identified and removed prior to analysis.

First, we analyze the distributional differences of the urban centers between the Global North and the Global South on the environmental, geographic, social, and economic indicators to provide the basis for further analysis. The Mann–Whitney *U* test, a non-parametric method for non-normally distributed data, is employed. The method calculates statistics through ranked comparisons and assesses the significance of the difference in terms of *p*-value. Its advantage is that it requires fewer assumptions about the distribution of the data and can effectively deal with outliers and asymmetric distribution.

Then, we analyze the relative importance of the three environmental indicators to identify their contributions to overall environmental development and compare these between the Global North and the Global South. To differentiate the relative status of the three environmental indicators, we employ a ternary diagram to partition the different roles of the three environmental indicators with their relative proportion (Fig. 6). Three vertices of the triangle are CO₂, PM_{2.5}, and greenness. The coordinate axes increase in a counterclockwise direction. For the conceptual diagram, each dimension is assigned an equal threshold of 1/3, producing a symmetrical and easily interpretable partition of the compositional space. This visual logic draws inspiration from soil texture ternary diagrams in soil science, where the relative proportions of sand, silt, and clay determine soil classification. In soil science, these thresholds are empirically derived from physicochemical properties at inflection points. Here, we adapt the method as a form of knowledge transfer to the urban environmental inequality context, assigning equal weight to the three dimensions in the absence of established visual conventions. For the empirical analysis, the observed mean values of each indicator were used to divide the triangle into six sectors: “high destruction area”, “high victimization area”, “high contribution area”, “destruction and victimization trade-off area”, “contribution and victimization trade-off area”, “destruction and contribution trade-off area”. The location and size of these six areas can be used to assess the relative environmental status of each urban center and compare them between Global North and Global South.

We use 2015 (or 2014) values for CO₂, greenness, and PM_{2.5}. CO₂ and PM_{2.5} are converted to per capita values, and per capita CO₂ is log-transformed to address non-normality. To eliminate dimensional differences and ensure data comparability, CO₂ emissions, PM_{2.5} concentration, and greenness are normalized. Subsequently, the three indicators are

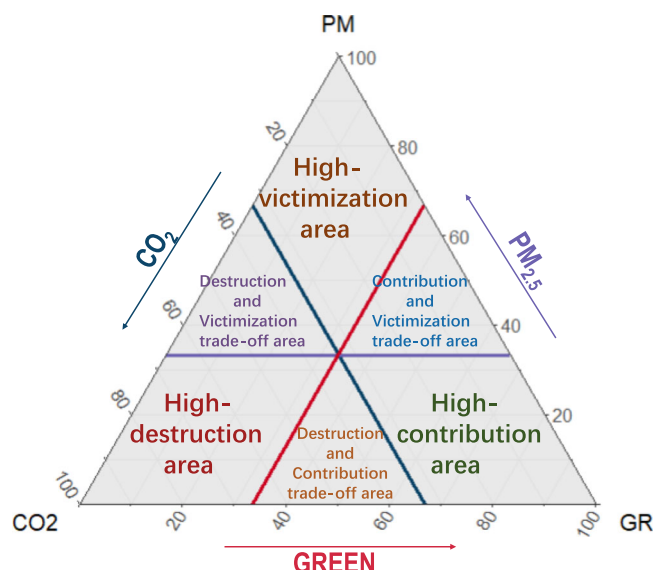


Fig. 6 | Conceptual ternary diagram of three environmental indicators of the urban centers. The blue, purple, and red arrows indicate the axes of CO₂, PM_{2.5}, and greenness, respectively, with their one-third division lines; the diagram shows how urban centers are positioned across the three environmental roles, dividing the space into high-destruction, high-victimization, high-contribution, and trade-off areas.

aggregated to calculate the proportion of CO₂ emissions, PM_{2.5} concentration, and greenness for each urban center, thereby deriving the relative proportions of these indicators. Finally, the relative proportions of the urban centers are mapped onto a ternary plot to visualize the balance among CO₂ emissions, air quality, and greenness across six areas.

Following that, we analyze the temporal changes of the three environmental indicators of the urban centers between the Global North and the Global South to identify if they are improved/degraded. The temporal changes are analyzed between 2000 and 2015, with 2000 when environmental governance started globally and 2015 when the most updated data were available. The findings can assist in identifying the urban centers where the most urgent actions should be taken. The environmental improvements are calculated as follows:

For CO₂ emissions and PM_{2.5} concentration:

$$\Delta X = \frac{X_{t1} - X_{t2}}{X_{t1}} \tag{3}$$

For greenness:

$$\Delta X = \frac{X_{t2} - X_{t1}}{X_{t1}} \tag{4}$$

Where: ΔX represents the percentage improvement of the environmental indicator, X_{t1} is the value of the indicator in the year 2000, X_{t2} is the value of the indicator in the year 2015.

We use a three-dimensional (eight quadrants) diagram to map the distribution of urban centers in different scenarios of environmental improvements/degradation together with their per capita GDP and population size. Each indicator is scaled between its 5th and 95th percentiles to reduce the influence of extreme values and improve comparability across regions. Among the eight scenarios, except the first quadrant in which the three indicators are all improved, we consider the priority order of future actions among the three environmental indicators as greenness, then PM_{2.5}, the third CO₂ emission based on their environmental roles and interactions between them. This prioritization is justified by several lines of evidence and economic considerations. First, enhancing greenness, besides its positive contribution to ecosystems and human health, plays a dual role in

environmental management by contributing to both CO₂ sequestration and PM_{2.5} reduction⁶⁰. Second, policy measures specifically targeting PM_{2.5} pollution have been shown to yield significant reductions in CO₂ emissions as a co-benefit. In contrast, initiatives that focus exclusively on CO₂ reduction do not effectively lower PM_{2.5} concentrations. Third, from an economic perspective, the financial investment required for PM_{2.5} mitigation is considerably lower compared to that needed for substantial CO₂ emission reductions^{49,61}. The eight quadrants are ranked as Quadrant I with the lowest mitigation efforts while Quadrant VIII with the highest mitigation efforts. Other quadrants are between.

Finally, we explore the difference in driving patterns of the environmental development of the urban centers between the Global South and the Global North to identify the causative chains (paths) of global urban environmental degradation. SEM is selected for its ability to simultaneously evaluate multiple interrelated pathways and integrate both latent and observed variables, making it particularly well-suited for analyzing the complex interactions within urban environmental systems. Specifically, SEM incorporates temperature, precipitation, and elevation as geographical variables; population, total built-up area, and prosperity as social variables; GDP and income group classifications as economic variables; CO₂ emissions as environmental destruction (cost); PM_{2.5} level as the indicator of environmental victimization (harm); and greenness as a measure of environmental contribution (benefit). The dataset was first standardized (z-score normalization) to remove unit effects and improve comparability across variables. Population, GDP per capita, and urban built-up area were natural log-transformed. Methodologically, we employed a piecewise SEM framework (implemented with mixed-effects models) to disentangle the causal pathways linking multiple environmental indicators with their socio-economic and geographic drivers. This application remains rare in large-scale global datasets covering more than 10,000 cities. The model was iteratively refined by sequentially adding random effects and by adding or removing potential pathways. Refinement continued until two criteria were met: (1) all retained paths were statistically significant at $p < 0.05$, and (2) overall model adequacy was confirmed by Fisher's C statistic (non-significant p-value), indicating no substantial deviation from the observed data. Our piecewise SEM differs from traditional SEM in two important ways. First, instead of estimating a single global variance-covariance matrix across all variables, piecewise SEM evaluates each structural equation separately, allowing the inclusion of random effects and nonlinear terms. This makes it possible to accommodate the hierarchical nature and large sample size of our dataset (>10,000 cities), but it also means that conventional global fit indices such as CFI and RMSEA cannot be computed in this framework. Second, in line with established practice in ecology and environmental science^{62,63}, we assessed model adequacy using Fisher's C statistic, which is specifically designed for piecewise SEM. The results were as follows:

Fisher's C = 1.769, df = 4, $p = 0.778$ (sample size = 1613)

Fisher's C = 3.415, df = 8, $p = 0.906$ (sample size = 10070)

In both cases, the high p-values indicate that the hypothesized causal structure does not significantly deviate from the observed data, suggesting an acceptable fit. Then we compared the models between the Global North and the Global South.

Data availability

All data used in this study are publicly available. The Global Human Settlement Urban Centre Database (GHS-UCDB) is provided by the European Commission's Joint Research Centre and can be accessed at https://human-settlement.emergency.copernicus.eu/ghs_stat_ucdb2015mt_r2019a.php.

Code availability

Model estimation was conducted in R (version 4.4.0) using the glmmTMB and nlme packages to fit individual component models, and the piecewiseSEM package to integrate them into a single SEM framework. The custom

code used for data processing and model analysis is publicly available at <https://github.com/weii20230124/Multiple-environmental-inequalities.git>.

Received: 4 April 2025; Accepted: 7 November 2025;

Published online: 24 November 2025

References

- Schell, C. J. et al. The ecological and evolutionary consequences of systemic racism in urban environments. *Science* **369**, eaay4497 (2020).
- Meng, J. et al. The rise of South-South trade and its effect on global CO₂ emissions. *Nat. Commun.* **9**, 1871 (2018).
- Keeler, B. L. et al. Social-ecological and technological factors moderate the value of urban nature. *Nat. Sustain.* **2**, 29–38 (2019).
- Bettencourt, L. M. A., Lobo, J., Helbing, D., Kuehnert, C. & West, G. B. Growth, innovation, scaling, and the pace of life in cities. *Proc. Natl. Acad. Sci. Usa.* **104**, 7301–7306 (2007).
- Arvidsson, M., Lovsjoe, N. & Keuschnigg, M. Urban scaling laws arise from within-city inequalities. *Nat. Hum. Behav.* **7**, 365 (2023).
- Balland, P.-A. et al. Complex economic activities concentrate in large cities. *Nat. Hum. Behav.* **4**, 248–254 (2020).
- Freeman, A. The geopolitical economy of international inequality. *Dev. Change* **55**, 3–37 (2024).
- Zhou, Y. et al. Satellite mapping of urban built-up heights reveals extreme infrastructure gaps and inequalities in the Global South. *Proc. Natl. Acad. Sci. Usa.* **119**, e2214813119 (2022).
- Li, Y. et al. Green spaces provide substantial but unequal urban cooling globally. *Nat. Commun.* **15**, 7108 (2024).
- Lim, C.-H., Ryu, J., Choi, Y., Jeon, S. W. & Lee, W.-K. Understanding global PM_{2.5} concentrations and their drivers in recent decades (1998–2016). *Environ. Int.* **144**, 106011 (2020).
- Stoddard, I. et al. Three Decades of Climate Mitigation: Why Haven't We Bent the Global Emissions Curve?. *Annu. Rev. Environ. Resour.* **46**, 653–689 (2021).
- Okereke, C. & Coventry, P. Climate justice and the international regime: before, during, and after Paris. *Wiley Interdiscip. Rev.-Clim. Change* **7**, 834–851 (2016).
- Akizu-Gardoki, O. et al. Hidden Energy Flow indicator to reflect the outsourced energy requirements of countries. *J. Cleaner Prod.* **278**, <https://doi.org/10.1016/j.jclepro.2020.123827> (2021).
- Chen, J., Huang, X., Shao, Z., Zheng, X. & Cai, B. Global Inequality of PM_{2.5} Exposure and ecological possession over 2001–2020. *J. Remote Sens.* **5**, <https://doi.org/10.34133/remotesensing.0446> (2025).
- Davide, D. F., Alessandra, F. & Roberto, P. Distributive justice in environmental health hazards from industrial contamination: a systematic review of national and near-national assessments of social inequalities. *Soc. Sci. Med.* **297**, 114834 (2022).
- Cohen, R. L. Distributive justice: theory and research. *Soc. Justice Res.* **1**, 19–40 (1987).
- Xu, C. et al. Global PM_{2.5} exposures and inequalities. *npj Clim. Atmos. Sci.* **8**, 54 (2025).
- Li, W., Chen, Z., Li, M. & Wen, Y. Technological progress accelerates CO₂ emissions peaking in a megacity: evidence from Shanghai, China. *Sust. Cities Soc.* **120**, <https://doi.org/10.1016/j.scs.2025.106150> (2025).
- Nagendra, H., Bai, X., Brondizio, E. S. & Lwasa, S. The urban south and the predicament of global sustainability. *Nat. Sustain.* **1**, 341–349, <https://doi.org/10.1038/s41893-018-0101-5> (2018).
- Chen, L., Chen, M., Zhang, X. & Xian, Y. Evaluating inequality divides in urban development intensity between the Global North and South. *Land Use Pol.* **145**, <https://doi.org/10.1016/j.landusepol.2024.107291> (2024).
- Cheng, W. et al. Global monthly gridded atmospheric carbon dioxide concentrations under the historical and future scenarios. *Sci. Data* **9**, 83 (2022).

22. Zheng, X. et al. Drivers of change in China's energy-related CO₂ emissions. *Proc. Natl. Acad. Sci. USA* **117**, 29–36 (2020).
23. Betts-Davies, S., Barrett, J., Brockway, P. & Norman, J. Is all inequality reduction equal? Understanding motivations and mechanisms for socio-economic inequality reduction in economic narratives of climate change mitigation. *Energy Res. Soc. Sci.* **107**, 103349 (2024).
24. Dong, K., Hochman, G. & Timilsina, G. R. Do drivers of CO₂ emission growth alter overtime and by the stage of economic development? *Energy Policy* **140**, <https://doi.org/10.1016/j.enpol.2020.111420> (2020).
25. Lamb, W. F. et al. A review of trends and drivers of greenhouse gas emissions by sector from 1990 to 2018. *Environ. Res. Lett.* **16**, <https://doi.org/10.1088/1748-9326/abee4e> (2021).
26. Shindell, D. & Rogelj, J. Preserving carbon dioxide removal to serve critical needs. *Nat. Clim. Chang.* **15**, 452–457 (2025).
27. Chancel, L. Global carbon inequality over 1990–2019. *Nat. Sustain.* **5**, 931–938 (2022).
28. Li, J., Han, X., Jin, M., Zhang, X. & Wang, S. Globally analysing spatiotemporal trends of anthropogenic PM_{2.5} concentration and population's PM_{2.5} exposure from 1998 to 2016. *Environ. Int.* **128**, 46–62 (2019).
29. Yang, D. et al. Global distribution and evolution of urbanization and PM_{2.5} (1998–2015). *Atmos. Environ.* **182**, 171–178 (2018).
30. Behrer, A. P. & Heft-Neal, S. Higher air pollution in wealthy districts of most low- and middle-income countries. *Nat. Sustain.* **7**, 203–212 (2024).
31. Zhang, Q. et al. Transboundary health impacts of transported global air pollution and international trade. *Nature* **543**, 705–709 (2017).
32. Haaland, C. & van den Bosch, C. K. Challenges and strategies for urban green-space planning in cities undergoing densification: a review. *Urban. Urban Green.* **14**, 760–771 (2015).
33. Zhang, Y., Ge, J., Wang, S. & Dong, C. Optimizing urban green space configurations for enhanced heat island mitigation: A geographically weighted machine learning approach. *Sust. Cities Soc.* **119**, <https://doi.org/10.1016/j.scs.2024.106087> (2025).
34. Yin, Y., He, L., Wennberg, P. O. & Frankenberg, C. Unequal exposure to heatwaves in Los Angeles: Impact of uneven green spaces. *Sci. Adv.* **9**, <https://doi.org/10.1126/sciadv.ade8501> (2023).
35. Han, Y., He, J., Liu, D., Zhao, H. & Huang, J. Inequality in urban green provision: a comparative study of large cities throughout the world. *Sust. Cities Soc.* **89**, 104229 (2023).
36. Brenner, N. *Implosions/Explosions: Towards a Study of Planetary Urbanization* (Jovis, 2014).
37. Roy, A. Slumdog cities: rethinking subaltern urbanism. *Int. J. Urban Reg. Res.* **35**, 223–238 (2011).
38. Hickel, J., Dorninger, C., Wieland, H. & Suwandi, I. Imperialist appropriation in the world economy: Drain from the global South through unequal exchange, 1990–2015. *Glob. Environ. Change-Human Policy Dimens.* **73**, <https://doi.org/10.1016/j.gloenvcha.2022.102467> (2022).
39. Amin, S. Unequal development: An essay on the social formations of peripheral capitalism. *Sci. Soc.* **42** (1978).
40. Bai, T., Qi, Y., Li, Z. & Xu, D. Digital economy, industrial transformation and upgrading, and spatial transfer of carbon emissions: The paths for low-carbon transformation of Chinese cities. *J. Environ. Manage.* **344**, <https://doi.org/10.1016/j.jenvman.2023.118528> (2023).
41. Yang, Y., Zhou, Y., Shan, Y. & Hubacek, K. The shift of embodied energy flows among the Global South and Global North in the post-globalisation era. *Energy Econ.* **131**, <https://doi.org/10.1016/j.eneco.2024.107408> (2024).
42. Cumming, G. S. et al. Implications of agricultural transitions and urbanization for ecosystem services. *Nature* **515**, 50–57 (2014).
43. Cumming, G. S. & von Cramon-Taubadel, S. Linking economic growth pathways and environmental sustainability by understanding development as alternate social-ecological regimes. *Proc. Natl. Acad. Sci. USA.* **115**, 9533–9538 (2018).
44. Sulemana, I., James, H. S. & Rikoon, J. S. Environmental Kuznets Curves for air pollution in African and developed countries: exploring turning point incomes and the role of democracy. *J. Environ. Econ. Policy* **6**, 134–152 (2017).
45. Simone, A. Cities of the Global South. *Annu. Rev. Sociol.* **46**, 603–622 (2020).
46. Hadžić, F. Power of global north vs. global south; environmental and climate change policies of inclusion, inequalities, and fragility. *Humanit. Today Proc.* **3**, 27–47 (2024).
47. Li, G. et al. Global urban greening and its implication for urban heat mitigation. *Proc. Natl. Acad. Sci. USA.* **122**, <https://doi.org/10.1073/pnas.2417179122> (2025).
48. Adilkhanova, I., Santamouris, M. & Yun, G. Y. Green roofs save energy in cities and fight regional climate change. *Nat. Cities* **1**, 238–249 (2024).
49. Yang, H. et al. Multi-objective analysis of the co-mitigation of CO₂ and PM_{2.5} pollution by China's iron and steel industry. *J. Clean. Prod.* **185**, 331–341 (2018).
50. Dormann, C. F. et al. Methods to account for spatial autocorrelation in the analysis of species distributional data: a review. *Ecography* **30**, 609–628 (2007).
51. Beale, C. M., Lennon, J. J., Yearsley, J. M., Brewer, M. J. & Elston, D. A. Regression analysis of spatial data. *Ecol. Lett.* **13**, 246–264 (2010).
52. Griffith, D. A. & Peres-Neto, P. R. Spatial modeling in ecology: The flexibility of eigenfunction spatial analyses. *Ecology* **87**, 2603–2613 (2006).
53. Melchiorri, M. et al. The multi-temporal and multi-dimensional global urban centre database to delineate and analyse world cities. *Sci. Data* **11**, <https://doi.org/10.1038/s41597-023-02691-1> (2024).
54. Zheng, H. et al. Control of toxicity of fine particulate matter emissions in China. *Nature* **643**, 404–411 (2025).
55. Brauer, M. et al. Global burden and strength of evidence for 88 risk factors in 204 countries and 811 subnational locations, 1990–2021: a systematic analysis for the Global Burden of Disease Study 2021. *Lancet* **403**, 2162–2203 (2024).
56. Agache, I. et al. Impact of residential greenness exposure on the development of allergic diseases and asthma and on asthma control—a systematic review for the EAAACI guidelines of environmental science for allergic diseases and asthma. *Allergy*, <https://doi.org/10.1111/all.16653> (2025).
57. Guo, G., Liu, L. & Duan, Y. Evaluating the association of regional and city-level environmental greenness and land over patterns with PM_{2.5} pollution: evidence from the Shanxi Province, China. *Front. Environ. Sci.* **10** (2022).
58. Shi, Y. et al. Assessment methods of urban system resilience: From the perspective of complex adaptive system theory. *Cities* **112**, <https://doi.org/10.1016/j.cities.2021.103141> (2021).
59. Zhai, G. et al. Nighttime light metrics for analysing urban-rural economic disparities: a case study in 36 Chinese metropolitan areas. *Cities* **162**, 105930 (2025).
60. Lin, H. & Jiang, P. Analyzing the phased changes of socioeconomic drivers to carbon dioxide and particulate matter emissions in the Yangtze River Delta. *Ecol. Indic.* **140** (2022).
61. Anenberg, S. C. et al. Particulate matter-attributable mortality and relationships with carbon dioxide in 250 urban areas worldwide. *Sci. Rep.* **9**, <https://doi.org/10.1038/s41598-019-48057-9> (2019).
62. Lefcheck, J. S. PIECEWISESEM: Piecewise structural equation modelling in R for ecology, evolution, and systematics. *Methods Ecol. Evol.* **7**, 573–579 (2016).
63. Shipley, B. Confirmatory path analysis in a generalized multilevel context. *Ecology* **90**, 363–368 (2009).

Acknowledgements

The authors would like to acknowledge the support from the National Natural Science Foundation of China (Grant No. 42230113 and 42171396); and the China Scholarship Council (Grant No. 202306190184).

Author contributions

W.L. and K.Y. data extraction; Y.W., W.L., L.C., and Z.C., conceptualization; Y.W., L.C., W.L., and Z.C., methodology; W.L. and D.X., processing and empirical analysis; W.L., W.C., and D.X. software; W.L., W.C., K.Y., and Q.Z. visualization; W.L., Y.W., and L.C., writing—original draft; W.L., Y.W., and L.C., writing—review & editing; Y.W., Z.C., and M.L. supervision. Wei Li (W.L.); Yongping Wei (Y.W.); Lijuan Chen (L.C.); Zhenjie Chen (Z.C.); Manchun Li (M.L.); Wenqi Chen (W.C.); Kunshu Yang (K.Y.); Diandian Xu (D.X.); Qiqi Zhao (Q.Z.)

Competing interests

The authors declare no competing interests.

Additional information

Correspondence and requests for materials should be addressed to Yongping Wei, Zhenjie Chen or Manchun Li.

Reprints and permissions information is available at <http://www.nature.com/reprints>

Publisher's note Springer Nature remains neutral with regard to jurisdictional claims in published maps and institutional affiliations.

Open Access This article is licensed under a Creative Commons Attribution-NonCommercial-NoDerivatives 4.0 International License, which permits any non-commercial use, sharing, distribution and reproduction in any medium or format, as long as you give appropriate credit to the original author(s) and the source, provide a link to the Creative Commons licence, and indicate if you modified the licensed material. You do not have permission under this licence to share adapted material derived from this article or parts of it. The images or other third party material in this article are included in the article's Creative Commons licence, unless indicated otherwise in a credit line to the material. If material is not included in the article's Creative Commons licence and your intended use is not permitted by statutory regulation or exceeds the permitted use, you will need to obtain permission directly from the copyright holder. To view a copy of this licence, visit <http://creativecommons.org/licenses/by-nc-nd/4.0/>.

© The Author(s) 2025